ELSEVIER

Journal of Structural Geology 27 (2005) 2223–2233

JOURNAL OF STRUCTURAL GEOLOGY

www.elsevier.com/locate/jsg

Determination of fabric and strain ellipsoids from measured sectional ellipses—implementation and applications

Patrick Launeau[a], Pierre-Yves F. Robin[b,*]

[a]*Laboratoire de Planétologie et Géodynamique, Université de Nantes, Faculté des Sciences et des Techniques, 2, rue de la Houssinière, 44072 Nantes, France*
[b]*Department of Geology, Earth Sciences Centre, University of Toronto, 22 Russell Street, Toronto, ON, Canada M5S 3B1*

Received 12 October 2004; received in revised form 9 July 2005; accepted 2 August 2005
Available online 15 September 2005

Abstract

Geologists examine fabrics to constrain models of formation or of deformation of rocks, and it is often convenient to summarise the results by a fabric ellipsoid. As fabric data are commonly collected on planar sections through the rock, estimating a fabric ellipsoid from sectional ellipses, often with arbitrary orientations, is an important task. An algebraic method to calculate such an ellipsoid, presented in an earlier paper, has been implemented with the program ELLIPSOID. It is used here on examples that illustrate questions and issues that arise when collecting, selecting and processing sectional fabric data, and when assessing the results. The quality of fit of the ellipsoid to the data is assessed in all cases. Examples include a case in which the average sizes of markers on individual sections can be used in the determination of the ellipsoid, and other cases in which such sizes are not useful; a case in which sectional ellipses are not obtained from closed markers; and a case in which data scatter and insufficient coverage of section orientations lead to a hyperboloid instead of an ellipsoid.
© 2005 Elsevier Ltd. All rights reserved.

Keywords: Sectional fabric ellipse; Fabric ellipsoids; Sectional ellipses; Strain analysis

1. Introduction

Geologists often seek to obtain three-dimensional fabric information from rocks, although many fabric data are collected on two-dimensional sections. As in the type example of paleostrain determination, whenever sectional fabric data can be represented or summarized by an ellipse and the sought three-dimensional fabric by an ellipsoid, it is necessary to calculate the ellipsoid from measured sectional ellipses. Robin (2002) presented an algebraic solution to the problem of fitting an ellipsoid from three or more sectional ellipses of arbitrary orientations. The method is implemented in ELLIPSOID,[1] a Visual Basic program, and we present here several examples that illustrate its use and some of the issues that arise when seeking a best-fitting fabric ellipsoid.

Robin (2002) developed two solutions to determine a best-fitting ellipsoid. In 'Case 1', 'with scale factor', the average size of markers on individual sections is deemed significant and contributes to determination of the ellipsoid. Indeed, in the field, a geologist commonly uses average marker sizes to approximate fabric directions. One may, for example, search sections on which average markers size is smallest as an approximation of the normal to the shape lineation direction; or, on the contrary, one might search for the largest marker size to find the foliation. In Case 1, the data collected on each of three or more sections are typically the orientation of the long axis of the sectional ellipse, and the sizes of its long and short diameters. Sectional data, including the actual dimensions of sectional markers, are used to build the components of a system of six linear equations in the six unknown coefficients describing the ellipsoid.

In 'Case 2', 'without scale factor', individual sections do not yield any useful size information. This may be because the number of markers on each individual section is too small to give a meaningful indication of average size, or sizes of the 3D markers are too variable, or the method to

* Corresponding author. Tel.: +1 416 978 5080; fax: +1 416 978 3938.
E-mail addresses: patrick.launeau@chimie.univ-nantes.fr (P. Launeau), py.robin@utoronto.ca (P.-Y.F. Robin).

[1] ELLIPSOID can be downloaded as freeware from http://www.sciences.univ-nantes.fr/geol/UMR6112/SPO/.

0191-8141/$ - see front matter © 2005 Elsevier Ltd. All rights reserved.
doi:10.1016/j.jsg.2005.08.003

determine a sectional ellipse does not yield any size. The only data retained are then orientation and axial ratio of each sectional ellipse. Given N sections, the data are used to build the components of a system of $(N+5)$ equations in $(N+5)$ unknowns: N 'scale factors' (one for each section) and five independent parameters that define a dimensionless ellipsoid.

In both Cases 1 and 2, solution of the system of equations corresponds to minimizing a scalar 'incompatibility index', $\sqrt{\bar{F}}$, which is a measure of the misfit between sectional ellipses and the ellipsoid sought (Robin, 2002). As the system always yields a solution, regardless of quality and fit of the data, understanding the meaning of the incompatibility index is important in order to determine our confidence in the results. An incompatibility index, $\sqrt{F^I}$, is also calculated for each individual face I, and can therefore eventually be used to query and re-evaluate individual data.

As in the method of Owens (1984), ELLIPSOID implements the possibility of assigning different weights to different sections. Different weights can be assigned as a function of the different confidence in the data from each section (Robin, 2002) or because several sections, e.g. because of their similar orientations, are not considered to be sufficiently independent from each other (Owens, 1984).

In some cases, the quadratic surface that best fits the data is a single-sheet hyperboloid rather than an ellipsoid. This might arise in particular when the sectional data are scattered or of modest quality and there is no section parallel to the long axis of the fabric ellipsoid (i.e. parallel to the 'lineation'). It is important then to know what further data are needed to 'close' that hyperboloid.

Four examples presented here are selected to illustrate several aspects of fabric ellipsoid determination. (1) Owens (1984) was the first to establish a method to determine an ellipsoid from any number (≥ 3) of arbitrarily oriented sections. We apply ELLIPSOID to reduction spots analysed in one of Owens's examples and compare incompatibility indices. (2) Mafic enclaves near the border of the Mont-Louis provide an example where insufficient data yield a hyperboloid rather than the ellipsoid sought, and also show how individual incompatibility indices can be used to either track measurement errors or provide additional information on mechanisms of fabric acquisition. (3) The opaque aggregates studied in thin sections of the Tellnes ilmenite deposit of SW Norway provide an example of determination of sectional ellipses that are not determined from closed markers, and one in which the ellipsoid determined from sectional data can be compared with that obtained by measuring the anisotropy of magnetic susceptibility (AMS). (4) Pyroxene fabric in gabbro-norite from the Critical Zone, on the eastern limb of the Bushveld complex, is acquired from large numbers of grains on each section, for which we can compare the results obtained by using or not using measured scale factors. The last two examples also illustrate how practical 'resampling statistics' can document our confidence that the sample size from data sections is sufficient. For each example, we try to indicate the geological significance of the results.

Conventions used for data entered into ELLIPSOID and presented in Tables 1 and 3 (specifically the right-hand rule and the convention on orientation of rake of the long axis of the sectional ellipse) are given in Appendix A. The appendix also discusses coordinate system and the transformation from laboratory coordinates to geographic coordinates that ELLIPSOID can effect whenever convenient.

Table 1
Sizes and orientation of reduction spots on sections of a sample of Dinorwic slate, N. Wales. Data from Owens (1984)

No.	Strike	Dip	Rake	Long axis (mm)	Short axis (mm)	Weight	ρ_0-1	$\sqrt{F^I_{\min}}$ (%)
1	302	78	165	16.5	4.5	0.58	0.17	3.0
2	301	77	166	9.5	3.5	0.58	0.16	2.8
3	302	75	166	20.5	6.8	0.58	0.06	1.4
4	201	71	173	37	6	1	0.03	0.2
5	178	71	0	7.5	1.5	1	0.07	1.9
6	18	79	10	16.7	3	0.58	0.26	4.4
7	17	78	8	22	4	0.58	0.06	0.8
8	19	78	7	18	3	0.58	0.11	2.1

2. Owens's (1984) reduction spots in a slate from Dinorwic, N. Wales, UK

Owens (1984) measured reduction spots on eight sections cut through an unoriented block of slate (Table 1, columns 1–6). Each section only displays one spot. In an actual field project, an ellipsoid determined on an oriented sample could be used to assess the direction, style, and intensity of deformation within a slate belt.

Whereas one might expect reduction spots in a given rock to have similar sizes in three dimensions, size set by some characteristic diffusion distance, actual sections through them are in general not through their centres. Therefore, the size of one marker per section is not likely to carry useful strain information; only the calculation without scale factor (Case 2) is justified. Owens (1984) assigned weights to his measurements (Table 1, column 7), decreasing some on the basis of proximity of their directions to those of other sections. Fig. 1a shows the results using the same weights as Owens, whereas Fig. 1b is for equal weights assigned to all sections. With an incompatibility index of 2.0 and 2.1%, respectively, the fit is good. The effect of weighting is small, a consequence of the fact that sectional ellipses are closely compatible.

Table 1 (last column) lists the individual incompatibility indices for each spot. The index for Spot No. 6 is 4.4%. If that face is discarded, the total incompatibility index for the new determination is reduced to 1.6%, the trend of the long axis changes by 9° and A/C is reduced from 7.7 to 6.5

(Fig. 1c). Considering how small the data set is, these changes may be deemed small. Owens's (1984) best-fit solution, shown in Table 2, is essentially identical to the solution found with ELLIPSOID after elimination of Spot No. 6.

Owens (1984) calculates the equivalent of an incompatibility index for each section by applying to each sectional ellipse a virtual 'retrodeformation' defined by the ellipsoid found. This retrodeformed axial ratio, ρ_0^I, can be compared with that of a circle, i.e. to 1, or to the average value of these ratios for all sections. Owens's values of $\rho_0^I - 1$ are given in Table 1 (column 8). Plot of one incompatibility index vs. the other shows an approximate linear correlation between the two. The discussion by Owens (1984) on the use of such an index to identify 'rogue data' remains entirely appropriate for determinations with ELLIPSOID and will be reviewed again in the next example.

Table 2
Results of Owens (1984) for symmetry axes of ellipsoid calculated from sections of reduction spots in a slate sample from Dinorwic, N. Wales, UK; to be compared with results in Fig. 2a

	A	*B*	*C*
Normalized length	2.34	1.20	0.36
Trend (°)	29	122	265
Plunge (°)	10	14	73

3. Mafic enclaves in the hercynian Mont-Louis granite, eastern central Pyrenees

Geologists concerned with granite emplacement generally interpret shapes of enclaves found in granitic rocks as providing some record of deformation of these enclaves. However, that deformation does not relate simply to any well-defined strain in the host granite, and it is also expected

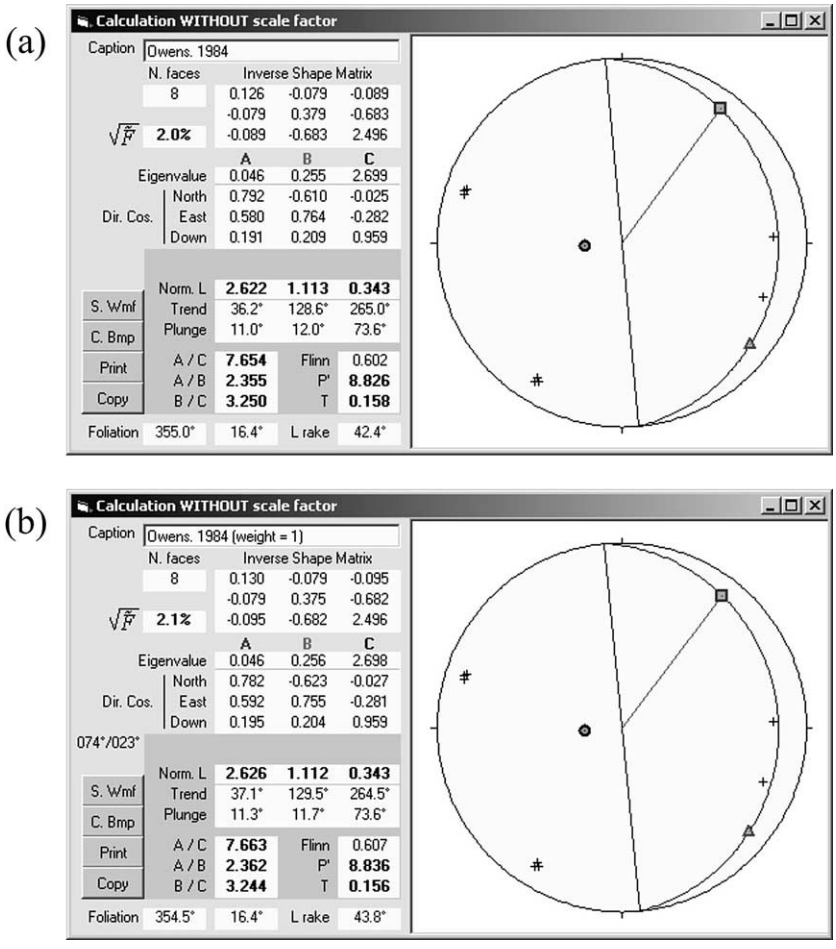

Fig. 1. Two outputs of ELLIPSOID for sectional data on reduction spots in slates from Dinorwic, N. Wales, UK. Data, from Owens (1984), are shown in Table 1. Each window shows the number of faces, *N*, used in the calculation, the coefficients of the inverse shape matrix calculated by the method of Robin (2002), eigenvalues of that matrix, direction cosines of the corresponding eigenvectors, the corresponding diameters of the best-fit ellipsoid normalized to $ABC = 1$, their directions given by their trends and plunges, axial ratios, strike and dip of the 'foliation' found, and rake of the 'lineation' within the foliation plane. 'Flinn' is the shape parameter, $(A/B-1)/(B/C-1)$; P' and T are, respectively, the intensity and shape parameters defined by Jelinek (1981) for the AMS tensor and applied here to the shape ellipsoid. The equal-area spherical projection shows the poles to the planar sections used (+), the directions of the long axis of the ellipsoid found (□), of its intermediate axis (△), and of its short axis (○), the plane of 'foliation' (i.e. plane A). (a) Ellipsoid found for sectional data weighted as by Owens (1984). See Table 1. (b) Ellipsoid found when all sections are weighted equally.

that different populations of enclaves may show different combinations of deformation and of rigid rotation, as recently emphasized by Paterson et al. (2004). Still, enclaves often exhibit a well-defined anisotropic distribution that must record some common history. We describe a sequence of measurements and results obtained in the field close to the southern contact of the Mont-Louis granite, near Site 10 of Gleizes et al. (1993, fig. 3).

Each oriented section measured is a rock face on which one enclave section is seen and, as with reduction spots, sectional areas of these enclaves are not expected to carry any useful size information: only sectional axial ratios and

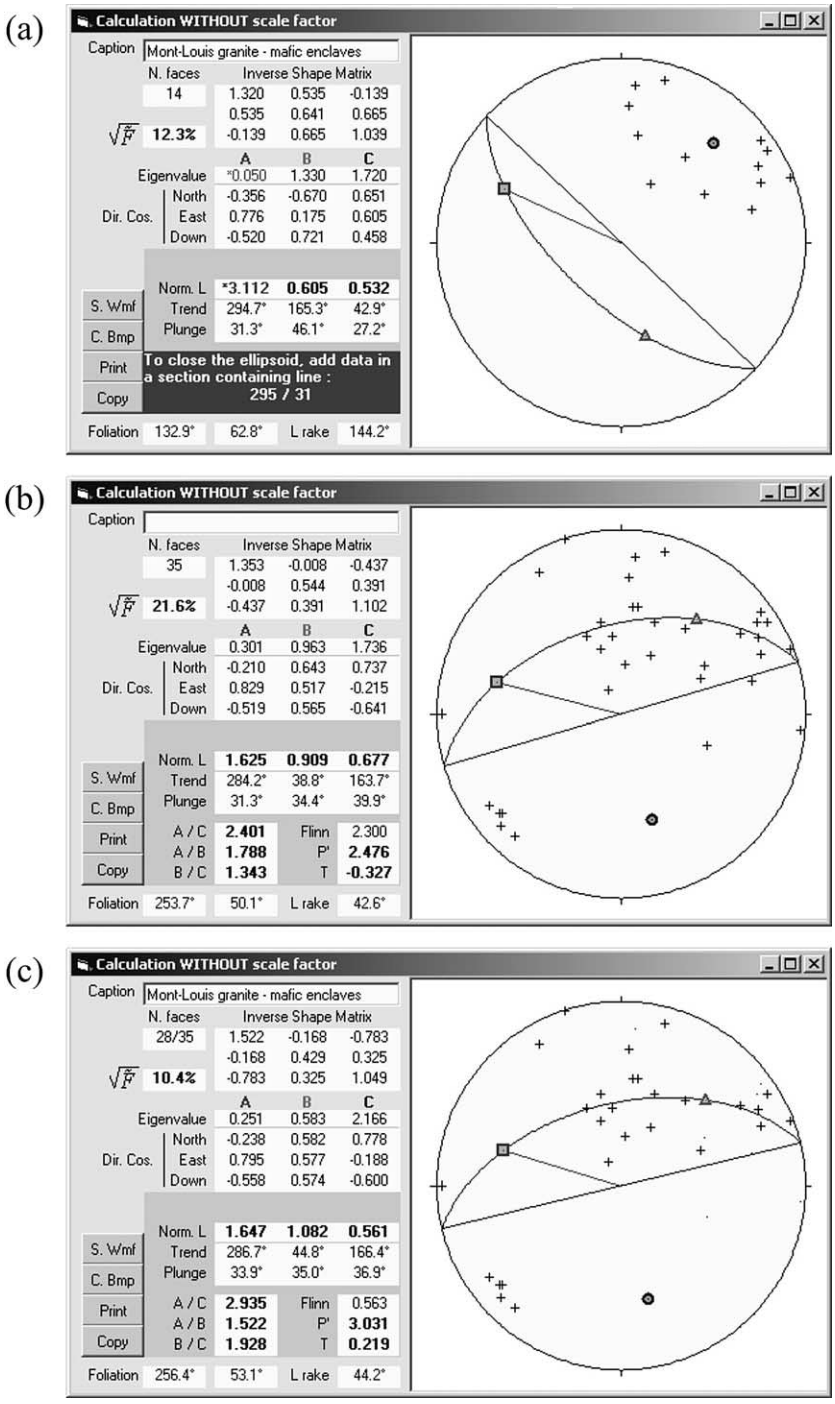

Fig. 2. Ellipsoid determinations from mafic enclaves in the Mont-Louis granite. (a) The first 14 enclaves measured yield a hyperboloid instead of an ellipsoid. (b) Ellipsoid obtained with 21 additional measurements. (c) Elimination of seven measurements with individual compatibility indices above 30% does not change the result much but decreases the overall incompatibility index.

directions are used to determine an ellipsoid (Case 2, 'without scale factor').

3.1. The 'hyperboloid problem'

The first 14 measurements, from a road-cut outcrop, were on rock faces with a relatively narrow range of orientations, shown by ELLIPSOID as poles (with a + symbol) in a lower hemisphere equal-area projection (Fig. 2). They yield one negative eigenvalue for the inverse-shape matrix describing the ellipsoid (Robin, 2002), indicating that the conic surface found is a single-sheet hyperboloid rather than an ellipsoid. The corresponding axial 'length', rather than shown as a complex number, is shown by ELLIPSOID in red and preceded by an asterisk (*). As explained below, finding a hyperboloid is not due to an algebraic failure: some data may fit a hyperboloid best.

Fig. 3a shows a model of three measured sectional ellipses with an insufficient coverage in their orientations. Sizes of the measured sections are assumed not to be a useful parameter, but they have been drawn here so that each area matches the area of their respective elliptical section of the conic surface found. It is intuitively easy to see that some distributions could fit a hyperboloid, and even do so with a low incompatibility index. Yet a hyperboloid, even though it might be a solution to the geometrical problem, is not an acceptable geological solution. If an additional, better-oriented face, such as Face 4 (Fig. 3b) is measured, it serves to 'close' the conic surface, and the calculation now yields an ellipsoid. In the authors' experience, the symmetry axis of the hyperboloid corresponding to the complex eigenvalue, shown as a square in Fig. 2a, is often close to the long direction of the ellipsoid that is found when more data are obtained.

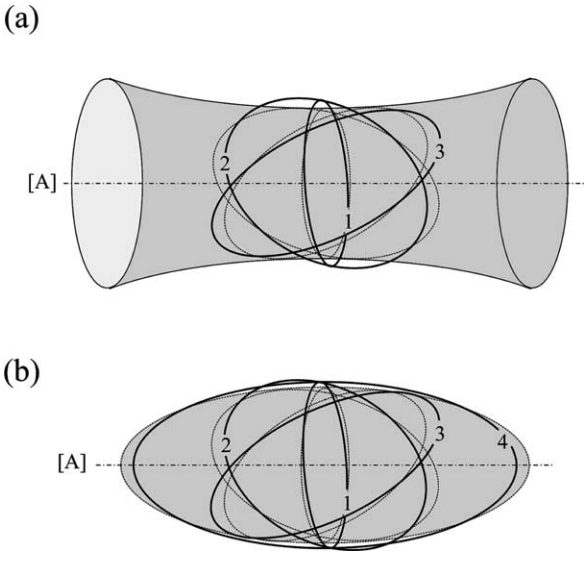

Fig. 3. (a) In some cases, the quadratic surface that best fits measured ellipses is a hyperboloid rather than an ellipsoid. (b) Additional data, particularly from planar sections close to the direction of the axis [*A*] of the hyperboloid, should 'close' the ellipsoid.

3.2. Incompatibility indices and elimination of outlying data

An additional 21 enclaves measured within 60 m of the original site yield the result shown in Fig. 2b, in which the long axis of the ellipsoid is indeed close to the 'complex axis' originally found and shown in Fig. 2a. Paradoxically, the incompatibility index, 21.6%, is larger than before (11.6%), no doubt a reflection of the complexity of fabric development in enclaves. Such an increase does not necessarily mean that our confidence in our estimate has decreased. This is because $\sqrt{\tilde{F}}$ can be thought of as an estimate of the *standard deviation* of the *population* of sectional ellipses. It describes that population itself. In analogy with the confidence in the *estimate* of a mean, and without any claim to statistical rigour, we may take our interval of confidence in the result as varying as $\sqrt{\tilde{F}/N}$, N being the number of sections measured. As it turns out, this ratio does increase slightly here, from 3.10 for the 14 measurements to 3.65 for the 35 measurements. In other words, our confidence has indeed decreased somewhat, supporting the suggestion that the population of enclaves is complex and somewhat heterogeneous.

Table 3 shows all 35 data and the calculated incompatibility index, $\sqrt{F^I_{\min}}$, for each face I. We note that the index for Face 18 is 82.3%. This may be treated as an exceptional outlier, and we investigate the effects of eliminating it (by assigning it a weight of 0). All individual incompatibility indices change somewhat; we can now eliminate the enclave with the next highest index. Repeating this procedure until all data with an index $>30\%$ are eliminated yields the results shown in Fig. 3d. After eliminating seven enclaves in this manner, the overall incompatibility index has decreased from 21.6 to 10.4%, the foliation and lineation directions have not changed significantly, but the Flinn parameter, $(A/B-1)/(B/C-1)$, has changed from 2.30 to 0.56. With this procedure, ellipsoid determination thus provides a tool and the data to investigate the competing mechanisms leading to a final enclave fabric as well as potential measurement errors (Owens, 1984), outliers can be examined, e.g. for petrographic characteristics or for shapes that are more or less likely to rotate than to deform passively, etc.

3.3. Mont-Louis marginal enclaves

As mentioned earlier, the site studied is near the southern margin of the Mont-Louis granite, where we would expect the latest magmatic strain to be dominantly shear parallel to the local direction of magma movement with respect to the wall. For this site, with $B=0.91$–1.08, i.e. close to 1, data are compatible with such magmatic strain (at least that part

Table 3
Measurements of enclaves near the south wall of the Mont-Louis Massif, East Central Pyrenees, by Patrick Launeau and Gérard Gleizes

I	Strike (°)	Dip (°)	Rake (°)	Long axis (cm)	Short axis (cm)	$\sqrt{F^I_{min}}$ (%)
1	99	49	170	11	2.5	24.4
2	93	63	155	13.5	2.5	19.5
3	93	63	157	5.5	2	10.7
4	151	74	133	7	2.5	11.1
5	159	88	127	18.5	6	21.9
6	157	71	122	5.5	2.5	11.2
7	166	62	140	6	1.2	35.3
8	148	83	134	4	0.9	19.8
9	150	43	145	6	1.7	31.7
10	95	74	139	5	1.5	28.3
11	105	80	154	3.5	1.6	5.5
12	144	83	154	8.5	1.6	37.9
13	127	48	152	7	1.8	20.7
14	117	29	152	3.7	1.6	5.5
15	321	74	50	10	5.1	13.6
16	320	73	51	8	2	28.2
17	325	76	49	6	2.8	15.4
18	146	78	20	11	1.3	82.3
19	0	87	60	40	18	24.9
20	317	78	53	6.5	2.1	24.8
21	311	77	44	13.5	4	19.2
22	83	35	0	14	5	18.5
23	72	30	5	5.5	2.2	16.7
24	66	38	10	2.8	1.7	4.7
25	60	78	25	19.5	8.7	36.3
26	96	49	170	7.5	2.2	20.1
27	200	41	47	7	2.8	44.0
28	146	67	129	6.5	2.7	7.2
29	61	12	0	6.2	2.8	30.4
30	156	39	115	34	9.5	15.0
31	72	90	7	6.5	2.5	33.0
32	77	42	0	12	4.1	19.3
33	110	44	140	4.3	1.2	26.4
34	95	22	159	15	6	18.2
35	185	87	56	13.7	4	74.1

of the strain responsible for the shape of the enclaves), with magma coming up from a west-north-west direction. The same orientation is found at a site with 48 enclaves located 11 km to the east along the same margin. This relatively simple and robust pattern suggests that late emplacement strain may still have played a dominant role in enclave shape fabric, in spite of the expected variety of enclave rigidities and deformation histories. This may be because the host magma in that final stage, close to the margin, was sufficiently crystallized for the viscosity contrast to be low, and was thus able to impose a significant strain on most enclaves.

4. Image analysis in the Tellnes Ilmenite deposit, SW Norway

The Tellnes ilmenite norite ore body of SW Norway is the second most important magmatic titanium deposit in production in the world. It is interpreted as a late dike (~920 Ma) within an anorthosite host. The ilmenite, actually a hemo-ilmenite (Duchesne, 1999), is interstitial to the sub- to euhedral crystals of plagioclase, orthopyroxene and olivine (see Fig. 4a). Its texture has been interpreted as a result of coalescence and recrystallization between the silicate minerals of earlier isometric-shaped ilmenite grains (Diot et al., 2003). In a study of the norite, Diot et al. (2003) compared the fabric of its opaque mineral phases, as obtained from sectional image analysis, with measured anisotropy of magnetic susceptibility (AMS). Sample TS 06 is reported here to illustrate the use of a sectional elliptic fabric that is based on interconnected rather than closed markers.

The determination of an ellipsoid from such a texture requires some discussion. If a section characterized by only two 'phases'—meaning here all opaque minerals vs. all non-opaque minerals—is isotropic, orientations of sectional boundaries are equally distributed over all orientations within the plane of the section. This means that a 'characteristic shape' for the image—which can be obtained in principle by sorting all boundaries according to their orientation and drawing them in sequence (e.g. Launeau and Robin, 1996, Section 4.5)—is a circle. In three dimensions, the characteristic shape would be a sphere and sectional characteristic shapes are sections of that sphere. If such a rock undergoes a homogeneous strain, the sphere becomes an ellipsoid, and sectional characteristic shapes become elliptical sections through that ellipsoid. Ellipsoid determination from sectional ellipses would therefore be no different here from that done where fabric elements are closed markers. More generally, any fabric element that can be used as a strain gauge can in principle give rise to sectional strain ellipses and to a strain ellipsoid determination. In the case of the Tellnes norite, the texture is not interpreted to be the result of an actual or of some virtual strain, and therefore the existence of an ellipsoidal characteristic shape in three dimensions is an approximation. But it is the same approximation as that for many closed markers that are not interpreted as strain markers.

4.1. Methodology

Samples were first analysed by AMS, using standard orientation procedures. Principal directions of the magnetic susceptibility tensor are shown on an equal-area projection in Fig. 4b. Large thin sections (3.25 cm×5 cm) were cut normal to these principal directions and labelled (*xy*), (*yz*) and (*xz*), according to the convention discussed in Appendix A. Although automated, the analysis of a site remains labour-intensive and three approximately orthogonal sections are a good choice that provides sufficient fabric information for the determination of a fabric ellipsoid

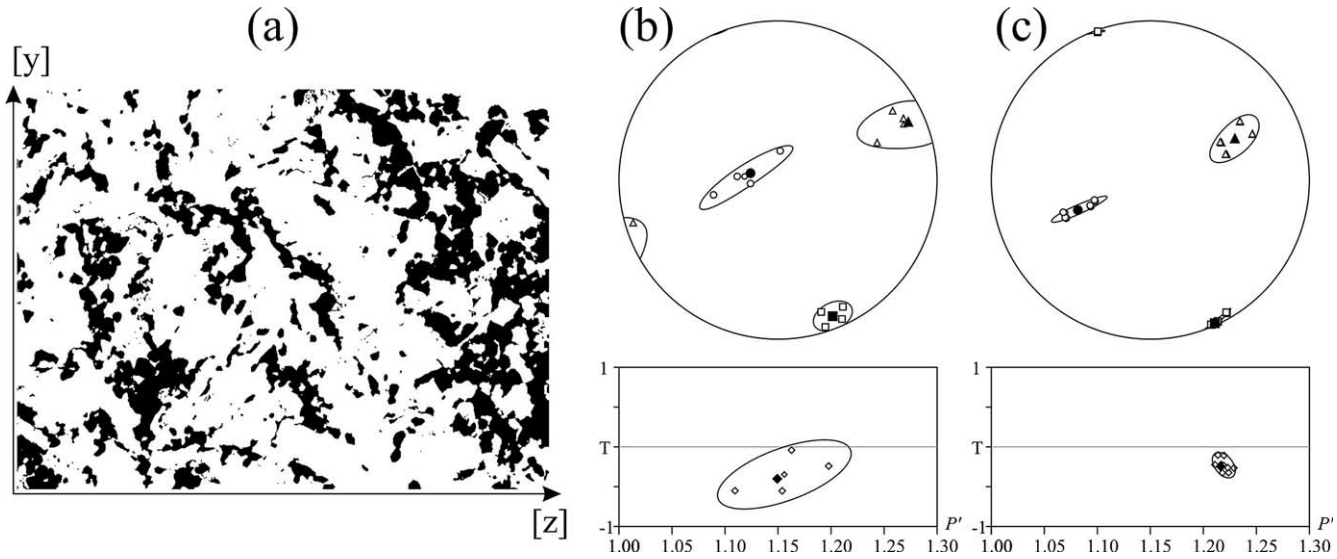

Fig. 4. Ilmenite + magnetite fabric in the Tellnes deposit, SW Norway. (a) Digital image of thin section, showing only opaque and non-opaque minerals. (b) Lower hemisphere equal-area spherical projection of the result of anisotropic magnetic susceptibility (AMS) measurements. Below it is the plot of Jelinek's parameters T vs P′. (c) Spherical projection showing orientation of the fabric ellipsoids calculated, with, below, Jelinek's parameters for the fabric ellipsoid found.

without undue thin section preparation and associated petrography.

In thin section, as shown in Fig. 4a, individual grains of interstitial ilmenite cannot be easily separated. Instead, boundaries between opaque minerals—with no distinction between ilmenite and magnetite—and non-opaque minerals were analysed with the method of intercepts (Launeau and Robin, 1996), using the latest version of the program INTERCEPT downloadable from the same page as ELLIPSOID. As discussed above, this method provides a record of the orientation distribution of the boundaries separating opaque from non-opaque phases and a sectional ellipse can be extracted from that record. The images do carry size information, but only the treatment without scale factor (Case 2) is reported here.

4.2. Scatter analysis and results

Fig. 4b shows the principal directions of AMS, with the traditional scatter of directions obtained from processing several samples. A comparable plot can be obtained from image analysis. The three large thin sections were each divided into halves, all halves were analysed separately, and the resulting sectional ellipses were combined in the eight different ways possible, thus yielding eight different ellipsoids. Fig. 4c shows the symmetry directions of these eight ellipsoids. We note that the scatter in the directions found is quite small, smaller than that of AMS; it indicates that the fabric is homogeneous over the scale of the large thin sections and that the sample size is sufficient. Directions found with AMS and image analysis of opaque minerals are in reasonable agreement, with all ellipsoid directions falling in the respective 2σ cones around the AMS mean principal directions. Even axial ratios are close, perhaps fortuitously: $k_1/k_2/k_3 = 1.08/0.98/0.94$, while $A/B/C = 1.11/0.99/0.91$. The incompatibility index for the ellipsoid is 1.6%, better than that for the reduction spots. This lower index is related not only to the large sampling provided by the intercept method, but is also a function of the low anisotropy of the fabric. A justifiable normalization of the incompatibility index to the anisotropy of the rock is yet to be devised.

Diot et al. (2003) argue that the directions found with AMS and with image analysis of opaque/non-opaque boundaries record the direction of the dike walls along which the noritic crystal mush was emplaced and the direction of magma flow within that fracture.

5. Pyroxene fabric in a gabbro-norite from the critical zone, eastern limb of the Bushveld complex

The ca. 2 Ga Bushveld complex is one of the world's largest deposits of base metals and platinum group elements. Yet the mechanism of emplacement and formation of its magmatic layers is still enigmatic. Fabric studies have been undertaken on a number of units within the complex in order to document a possible anisotropy within the plane of layering and therefore a possible magmatic flow direction. Using image analysis, Auréjac (2004) has analysed the pyroxene fabrics of

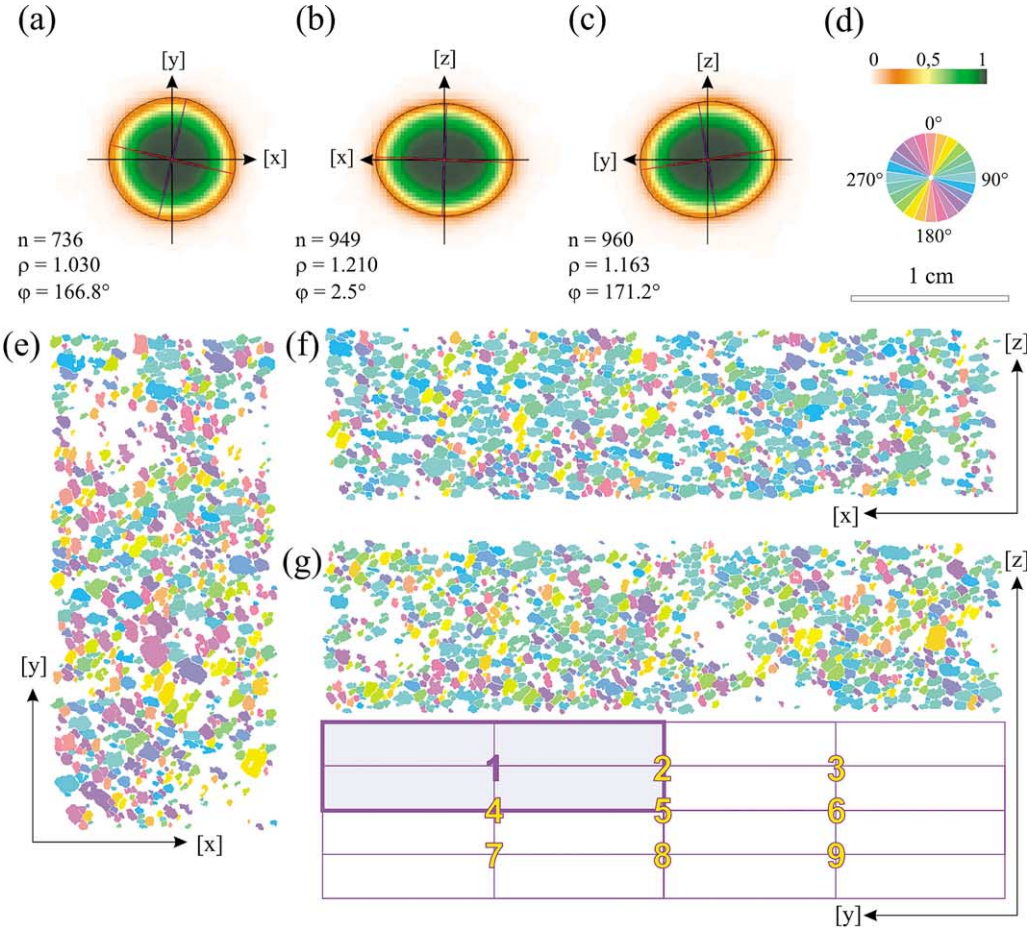

(h)

	A	B	C	$\sqrt{\widetilde{F}}$
L. norm	1.113	1.034	0.869	2.5%
trend	284.7	192.9	29.0	
plunge	5.1	19.1	70.2	
A/C	1.282		Flinn	0.405
A/B	1.077		P'	1.291
B/C	1.192		T	0.396

	A	B	C	729 combinations
L. norm	1.120	1.030	0.867	$\overline{X}$
	0.028	*0.033*	*0.021*	2σ
trend	285.9	194.2	29.1	$\overline{X}$
plunge	4.7	19.0	70.4	$\overline{X}$
	27.4	*27.4*	*8.8*	$2\sigma_1$
	5.6	*8.8*	*5.7*	$2\sigma_2$
	$\overline{X}$	2σ	$\overline{X}$	2σ
A/C	1.292	0.048	$\sqrt{\widetilde{F}}$ 2.6%	3.5%
A/B	1.087	0.057	P' 1.301	0.050
B/C	1.189	0.060	T 0.352	0.375

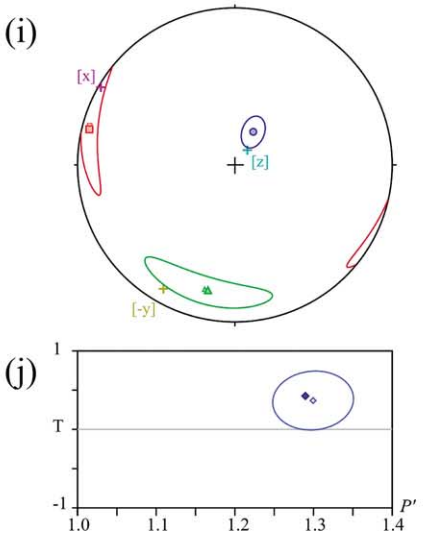

Fig. 5. Pyroxene fabric in a gabbro-norite from the critical zone, eastern limb of the Bushveld Complex. (a), (b) and (c) Number of pyroxene grains, n, used to calculate (by the inertia tensor method) the three orthogonal sectional ellipses shown, and parameters of the ellipses found. ρ, axial ratio of ellipse, ϕ, rake of long axis of ellipse, as defined by the convention shown in Fig. 7a. (e), (f) and (g) Digital images of the thin sections; the orientation of the long axis of each pyroxene grain is shown by its colour as per the rose in (d). The rectangle (1) of (g) is one example of nine quarter-size counting windows used to calculate 729 ($=9^3$) 'subset ellipsoids'. (h) Ellipsoid parameters calculated. (i) Lower hemisphere equal-area projection of the results. Solid symbols are for the 'full ellipsoid', i.e. that found by using all the pyroxene grains in each section. Open symbols are mean parameters of 729 'subset ellipsoids' (see text). Surrounding cone projections are at 2σ from each mean. For the two ellipsoids: squares indicate the long axes, A; triangles, B; circles, C. (j) T vs. P' for the same ellipsoids with previous mean and σ convention.

gabbronorite samples from 78 different sites spread northward from the vicinity of the Tweefontein mine over a north–south distance of ca. 60 km. No lineation is detected in the field. The analysis of Sample 50B is presented here to illustrate the use of scale factors in calculating the ellipsoid and to continue a reflection on statistical testing of the results.

5.1. Methodology of image analysis

The main fissility of the rock is subparallel to the layering. Each sample was therefore oriented in the field by marking and recording the orientation of its face parallel to that layering. The sample was then sectioned along three orthogonal cuts, one (*xy*) parallel to the layering and two, (*yz*) and (*xz*), normal to the layering and to each other (Fig. 5).

Oriented thin sections were then analysed on the rotating polarizer microscope developed by Fueten and Goodchild (2001). Orthopyroxene grains were identified and isolated by the same technique as that used by Fueten and Goodchild (2001) for quartz grains. The resulting images of individual grains are shown in Fig. 5e–g. Shape orientations of individual grains were determined by the inertia tensor method using program SPO (Launeau and Cruden, 1998; Launeau, 2004) downloadable from the same page as ELLIPSOID.

5.2. Results

Sectional results, without scale factor (Case 2), are shown in Fig. 5a–c, and the ellipsoid found, rotated back into geographic coordinates, is given in table form in Fig. 5h. The low value of the incompatibility index, 1.7%, is again a consequence of the low axial ratios of the faces and of the resulting ellipsoid as well as of the good fit. If the average sizes of the grains are used to provide a scale factor for each face and these scale factors are used in the calculation (Case 1), the results differ by less than 1% and by a fraction of a degree from the results shown here, while the incompatibility index increases to 2.2%. Thus, there is no significant difference between the results obtained by the two methods here.

The ratio *A*/*B* found within the plane of the layering is only 1.08. This is quite weak, which accounts for why no lineation could be seen in the field. In order to assess our confidence in the data, grains in each of the three sections were split into nine subsets by scanning a quarter size counting window in three staggered, evenly spaced positions along both the *x*- and *y*-directions; each subset contains around 230 grains. As was done for the Tellnes norite, subset ellipsoids are calculated from all possible combinations of sectional subsets, i.e. 729 ($=9^3$) ellipsoids, with each section weighted by its number of grains. Similar analysis with subsets is commonly used in mathematical morphology (Serra, 1982; Coster and Chermant, 1989). When each parameter of the 'full' ellipsoid (i.e. that calculated with all the data) falls within the 2σ intervals around the mean for the corresponding parameter of subset ellipsoids, we conclude that the size of the counting window is sufficient; the 2σ interval can then be seen as a confidence interval. On the contrary, when some or all the parameters of the full ellipsoid fall outside the 2σ range defined by subset ellipsoids, we conclude that the counting window is too small for the heterogeneity of the data. Such an ellipsoid usually displays a high global incompatibility index. The sensitivity of this technique increases with the number of subsets by the use of smaller counting windows and narrower scan steps, but a number of grains greater than 100 per subset is often necessary.

In the current example, the perfect match between the full and the subset ellipsoids (Fig. 5h–j) shows that even though the preferred orientation of the markers is weak, the directions of the axes of symmetry can be measured with high confidence. Auréjac (2004) finds that the lineation direction within the gabbro-norite layers is consistently WNW–ESE over the field area, whereas similar pyroxene grain lineation in the pyroxenite that underlies the gabbro-norite within each cycle is consistently NE–SW. Auréjac (2004) attributes the latter to primary emplacement direction of the magma in each cycle, and the former to secondary magma migration within the chamber.

6. Discussion and conclusion

As shown with these examples, calculation of ellipsoids from sectional ellipses is a tool that can provide valuable geological information such as direction of magma transport, of emplacement mechanism, or of deformation. Ellipsoid calculations should be equally interesting in studies of current direction, of paleoslope direction, or of diagenesis and compaction.

Individual incompatibility indices for each section are essential tools to assess the data. As already pointed out by Owens (1984), they can be used to search for errors in measurement or data entry. But also, as suggested with the Mont-Louis enclaves, identification of outliers may help document competing mechanisms of fabric acquisition. A global incompatibility index, $\sqrt{\bar{F}}$, is also essential, all the more necessary as the method always yields a result, regardless of whether the data are very compatible or very incompatible. But that index must not be interpreted too literally when comparing several data sets or comparing calculation methods. Modelling still needs to be done to evaluate how the incompatibility index varies as a function of the axial ratio.

There is at present no theory to translate the confidence intervals for the measurements on individual faces, and the distribution of face orientations into a confidence interval on the parameters describing the ellipsoid found. But partial sampling tests along the line of what was done for the

opaque grains in the Tellnes deposit and for the pyroxene grains in the Bushveld gabbronorite suggest a possible practical approach to this statistical problem.

In a recent paper, Gee et al. (2004) repeatedly assert that ellipsoid determinations from sectional ellipses require that sections be parallel to the symmetry directions of the fabric ellipsoid sought and also that absolute dimensions of the sectional ellipses must be known. These authors thus directly contradict several of the papers that they cite, including that of Robin (2002); as demonstrated here, both assertions are in fact incorrect. To find a remedy to what are in fact non-existent problems, Gee et al. (2004) propose to determine fabric ellipsoids by using the traces of planar crystallographic features (cleavage and exsolution lamellae in pyroxene grains, albite twin planes in plagioclase grains) on three orthogonal thin sections. They consider each such trace to approximate the projection on the section plane of the long direction of the grain; this is of course only true if the planar feature used happens to be perpendicular to that section, i.e. rarely, and never for all three sections. Still, it remains true that in an isotropic rock, such traces would be isotropically oriented in all sections and also true that if such directions are then assumed to rotate passively during a deformation, their distribution can be used to calculate a sectional strain. However, in this case, calculating a sectional ellipse from these data and from the resulting 'characteristic shape' (e.g. Launeau and Robin, 1996) for each section and combining sections with ELLIPSOID is a much simpler process than the multi-step and iterative method proposed by Gee et al. (2004).

Acknowledgements

We are grateful to Gérard Gleizes for his contribution to the collection of enclave data in the Mont-Louis granite, and to Jean-Baptiste Auréjac for sharing pyroxene shape data from the Bushveld and letting us refer to some of his conclusions. Reviews of versions of the manuscript by W.M. Schwerdtner, by Toshiko Shimamoto, and, particularly, by W.H. Owens lead to significant improvements of the paper. Jacques Girardeau helped make P.-Y.R.'s visits to Nantes, and consequently the project, possible. Part of the research was supported by the Canadian National Science and Engineering Research Council.

Appendix A

The orientation of each section is given by a strike, α, and a dip θ. In the right-hand rule used by ELLIPSOID, illustrated in Fig. A1, the strike is the azimuth of the strike line such that the dip of the plane is measured down from the right of that

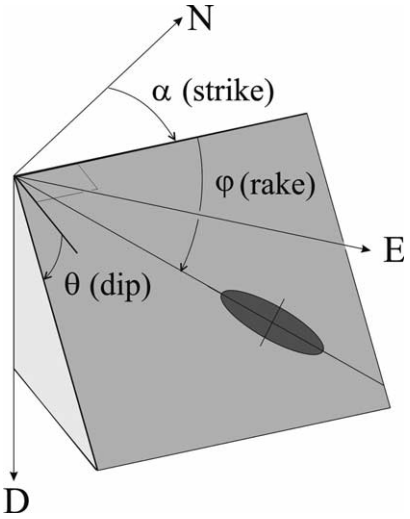

Fig. A1. Convention for the description of planes by strike (α) and dip (θ), and that of a direction within that plane by its rake (ϕ). A convention such as the one illustrated here is necessary for efficient and unambiguous entry of orientation data into a computer program. Although structural geologists would normally choose α between 0 and 360°, θ between 0 and 90° and ϕ between 0 and 180°, ELLIPSOID imposes no restriction on the signs and values of these angles that can be entered for them.

azimuthal direction. The strike is between 0 and 360°, counted clockwise from north. The dip θ can in principle be greater than 90° (e.g. as one may want to measure on an overhung face); but in Tables 1 and 3, dips are always smaller than 90°, and strike is chosen accordingly. The rake (/pitch) of the long axis of the sectional ellipse, ϕ, is the angle where the axis makes with the azimuthal line selected as per the above right-hand rule. Rake can vary between 0 and 180°. All calculations in ELLIPSOID assume a right-handed geographic coordinate system with [x] = north, [y] = east and [z] = down.

When making measurements on three orthogonal faces of a block in the laboratory, it is sometimes convenient instead to refer these measurements to an equally right-handed laboratory coordinate system [x], [y] and [z] (Fig. A2a). The transformation from the laboratory coordinate system to the geographic coordinate system is completely defined by a set of Euler angles corresponding to the strike α of the top face (xy) of the block, the dip θ of that face, and the rake ϕ of the laboratory [x] axis within that top face (Fig. A2b). If measurements on faces of the rectangular block are made in accordance with the reference directions shown in Fig. A2a and the above Euler angles are entered, ELLIPSOID can transform the orientation of the ellipsoid from lab coordinates to that in geographic coordinates. All Euler angles can have positive or negative values.

Alternatively, users can convert their sectional data to geographic coordinates before entering them into ELLIPSOID. A simple and practical way, particularly useful when the faces of the block are not orthogonal, is to set the block in a

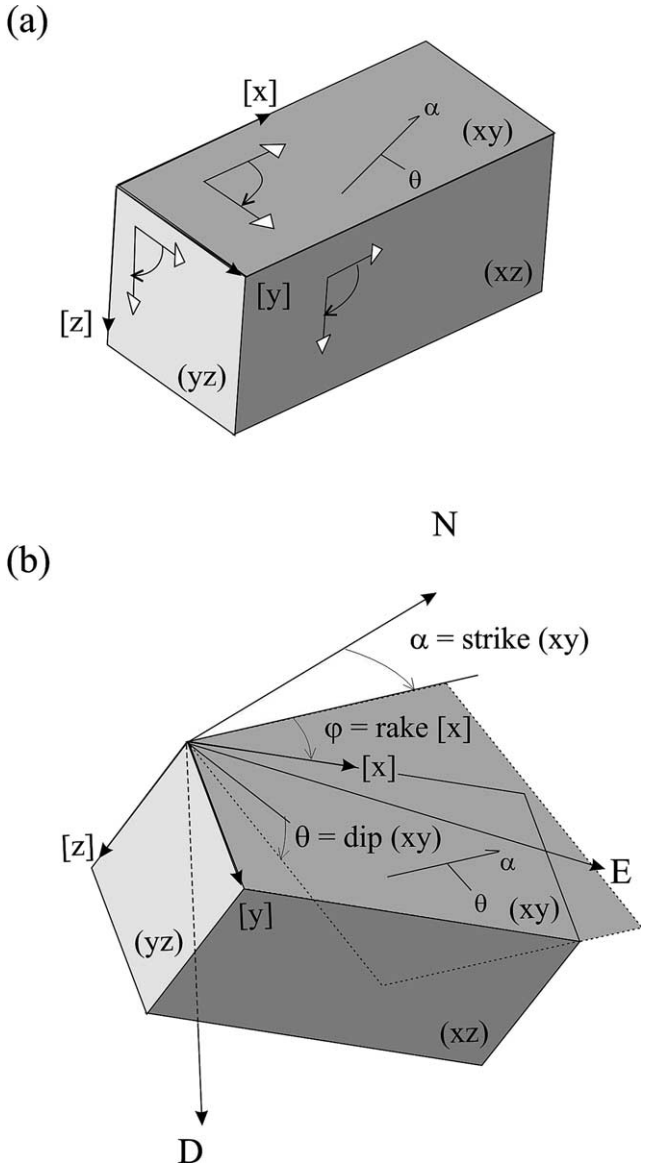

Fig. A2. (a) Sketch of the orientation conventions that can be used when measuring sectional ellipses and calculating fabric ellipsoid in three orthogonal sections in lab coordinates. (b) Complete characterization of the orientation of the (*xy*) face in geographic coordinates, indicated by the traditional strike and dip values, defines the parameters of the Euler matrix used by ELLIPSOID to rotate results back into geographic coordinates. Note that ϕ, the rake of the [*x*] direction in Face (*xy*), must be entered according to the convention defined in Fig. A1. In the case of the figure, ϕ is positive and less than 90°, and [*x*], [*y*] and [*z*] all point downward. For values of the various Euler angles that are negative or greater than 90°, one or more of the axes may point upward. Nevertheless, the rake ϕ of the [*x*] axis should always be measured clockwise when looking along the positive direction of [*z*].

sand box, re-orient it to its field orientation, using the preserved measured field face, and then measure the orientations of the faces and of the rakes with a compass and clinometer.

References

Auréjac, J.-B., 2004. Etude pétrostructurale de gabbros lités de la Zone Critique Supérieure, Complexe du Bushveld (Afrique du Sud). Thèse de doctorat, Université Paul Sabatier, Toulouse, France.

Coster, M., Chermant, J.L., 1989. Précis d'analyse d'images. Presse du CNRS, Paris. 560pp.

Diot, H., Bolle, O., Lambert, J.-M., Launeau, P., Duchesne, J.-C., 2003. The Tellnes ilmenite deposit (Rogaland, South Norway): magnetic and petrographic evidence for emplacement of a Ti-enriched noritic crystal mush in a fracture zone. Journal of Structural Geology 25, 481–501.

Duchesne, J.C., 1999. Fe–Ti deposits in the South Rogaland anorthosites (South Norway) geochemical characteristics and problems of interpretation. Mineralium Deposita 34, 182–198.

Fueten, F., Goodchild, J.S., 2001. Quartz *c*-axes orientation determination using the rotating polarizer microscope. Journal of Structural Geology 23, 895–902.

Gee, J.S., Meurer, W.P., Selkin, P.A., Cheadle, M.J., 2004. Quantifying three-dimensional silicate fabrics in cumulates using cumulative distribution functions. Journal of Petrology 45 (10), 1983–2009.

Gleizes, G., Nédélec, A., Bouchez, J.L., Autran, A., Rochette, P., 1993. Magnetic susceptibility of the Mont-Louis Andorra ilmenite-type granite (Pyrenees): a new tool for the petrographic characterization and regional mapping of zoned granite plutons. Journal of Geophysical Research 98 (B3), 4317–4331.

Jelinek, V., 1981. Characterization of the magmatic fabrics of rocks. Tectonophysics 79, 63–67.

Launeau, P., 2004. Mise en évidence des écoulements magmatiques par analyse d'images 2-D des distributions 3-D d'Orientations Préférentielles de Formes. Bulletin de la Société Géologique de France 175, 331–350.

Launeau, P., Cruden, A.R., 1998. Magmatic fabric acquisition mechanism in a syenite: results of a combined anisotropy of magnetic susceptibility and image analysis study. Journal of Geophysical Research 103, 5067–5089.

Launeau, P., Robin, P.-Y.F., 1996. Fabric analysis using the intercept method. Tectonophysics 267, 91–119.

Owens, W.H., 1984. The calculation of a best-fit ellipsoid from elliptical sections on arbitrarily orientated planes. Journal of Structural Geology 6 (5), 571–578.

Paterson, S.R., Pignotta, G.S., Vernon, R.H., 2004. The significance of microgranitoid enclave shapes and orientations. Journal of Structural Geology 26, 1465–1481.

Robin, P.-Y.F., 2002. Determination of fabric and strain ellipsoids from measured sectional ellipses—theory. Journal of Structural Geology 24, 531–544.

Serra, J., 1982. Image Analysis and Mathematical Morphology. Academic Press, London. 610pp.